

# Adaptive STBC MIMO-OFDM system design for indoor visible light communications

Guo Xinyue, Li Shuangshuang, Guo Yang, Xiao Jiangnan

(Shanghai Key Lab of Modern Optical System, School of Optical-Electrical and Computing Engineering,  
University of Shanghai for Science and Technology, Shanghai 200093, China)

**Abstract:** An adaptive multiple-input multiple-output orthogonal frequency division multiplexing (MIMO-OFDM) visible light communication(VLC) system based on space-time block coding (STBC) modulation was proposed in the paper, which can overcome the MIMO channel correlation and achieve reliable communications. Meanwhile, power-and-bit allocation(PBA) was combined with OFDM in order to adapt to the channel and improve the spectral efficiency. Then a 2×2 MIMO-OFDM VLC transmission over a distance of 80 cm was demonstrated, where the measured bit error rates were all below 7% of the pre-forward-error-correction threshold of  $3.8 \times 10^{-3}$ . Experimental results show that the STBC MIMO-OFDM system is robust to MIMO channel correlation, where the data rates can be greatly improved by applying the PBA.

**Key words:** visible light communication; space-time block coding;  
multiple-input multiple-output orthogonal frequency division multiplexing;  
power-and-bit allocation

**CLC number:** TN929.12    **Document code:** A    **DOI:** 10.3788/IRLA201847.0222001

## 室内可见光通信中的自适应 STBC MIMO-OFDM 系统设计

郭心悦,李双双,郭阳,肖江南

(上海理工大学 光电信息与计算机工程学院 上海市现代光学系统重点实验室,上海 200093)

**摘要:** 提出基于空时块码(STBC)调制的自适应多输入多输出正交频分复用(MIMO-OFDM)可见光通信(VLC)系统,该系统能够克服 MIMO 信道相关性并实现可靠通信。同时,引入功率比特分配(PBA)与 OFDM 相结合,以适应信道传输条件从而有效提高频谱效率。通过搭建一个 2×2 的 MIMO-OFDM VLC 演示系统,实现了 80 cm 距离的传输,实验中测得的误码率始终保持在 7% 的前向纠错阈值  $3.8 \times 10^{-3}$  之下。实验结果表明,STBC MIMO-OFDM 系统对 MIMO 信道相关性鲁棒,且 PBA 的应用能够大幅度提高数据速率。

**关键词:** 可见光通信; 空时块码; 多输入多输出正交频分复用; 功率和比特分配

收稿日期:2017-08-05; 修订日期:2017-10-03

基金项目:国家自然科学基金青年科学基金(61501296)

作者简介:郭心悦(1981-),女,讲师,博士,主要从事无线信号处理方面的研究。Email:xinyueguo@usst.edu.cn

## 0 Introduction

Visible light communication (VLC) based on white light emitting diodes (LEDs) has recently emerged as a compelling wireless communication technology beyond traditional radio frequency (RF) communications. Compared to traditional RF communications, VLC offers several advantages, including cost effectiveness, licensing free, immunity to electromagnetic interference, and high security<sup>[1]</sup>. The most severe challenge in achieving high-speed VLC transmission is its very limited modulation bandwidth, which is usually about several megahertz of the commercial LED<sup>[1-2]</sup>, resulting in serious inter-symbol interference (ISI) for high-speed transmission. Various VLC transmission strategies have been proposed to increase the communication capacity<sup>[3-5]</sup>, among which the orthogonal frequency division multiplexing (OFDM) scheme has been proved particularly useful for VLC system, because the channel can be decomposed into multiple frequency-flat sub-channels to eliminate ISI<sup>[6-7]</sup>. Another advantage is that OFDM has a large number of tunable parameters, and the system performance can be further improved by optimizing the communication parameters. Considering that the frequency response of VLC channel is non-flat, the well-known adaptive transmission technique power-and-bit allocation (PBA) is introduced in, which is combined with OFDM for adapting to the channel non-flat fading, and also improving spectral efficiency<sup>[8-9]</sup>.

On the other hand, since multiple LEDs are usually required to realize full-range illumination, multiple-input multiple-output (MIMO) becomes a promising technology in indoor VLC systems to provide better reliability and higher data rate without requiring additional frequency resources<sup>[10]</sup>. In the indoor MIMO VLC system design, one challenge stems from the high channel correlation, as the signals received by closely spaced receivers can be almost identical<sup>[11-12]</sup>.

Therefore, it would be difficult for receiver to separate the single data streams. Imaging MIMO<sup>[11]</sup> and angular diversity technique<sup>[12]</sup> have been proposed to deal with the channel correlation; however, precise alignment or auxiliary devices are required in these systems, which can limit their applications.

In this paper, space-time block coding (STBC) is proposed in the MIMO VLC system to overcome the channel correlation. STBC has already been proved to be robust to channel correlation in RF communication<sup>[13]</sup>. By coding across the space and time dimensions orthogonally, same information-bearing signals are sent from multiple LEDs over several time periods. In such a way, MIMO channel can be de-correlated and data streams can be separated by combining signals of both space and time dimensions. Therefore, STBC benefits for its high reliability and insensitivity to channel correlation. There have been researches in the STBC to offer highly reliable communications<sup>[14-16]</sup>; however, previous research did not consider the relationship between STBC and channel correlation. Moreover, in most pervious STBC designs for MIMO VLC system, only optical channels were considered, while the effect on LED frequency response was ignored.

The contribution of the paper is to build an adaptive MIMO-OFDM VLC system based on STBC modulation. First, the application of Alamouti STBC is investigated in MIMO-OFDM VLC system. Different from the existed works, the effect on LED frequency response is also considered in the Alamouti STBC design. Then, PBA is introduced to further improve the spectral efficiency by optimizing the parameters of OFDM modulation in the STBC based MIMO VLC system, where the power and bits are allocated to different sub-channels for maximizing the channel capacity. Finally, experimental demonstration is set up to study the performance of the proposed MIMO-OFDM VLC system. In the experiment, a MIMO configuration with 2 transmitters and 2 receivers is considered, and the measured bit error rates (BERs)

are all below the 7% pre-forward-error-correction (pre-FEC) threshold of  $3.8 \times 10^{-3}$  after 80 cm free-air transmission. Experimental results confirm that the STBC is robust to channel correlation and the data rates can be greatly improved by applying the PBA to the MIMO-OFDM system.

### 1 Principle

Alamouti STBC is a well-known MIMO scheme that combines both space and time diversity, which offers high reliability and is robust to channel correlation. In the Alamouti STBC scheme, symbols are transmitted from the two transmit LEDs over two symbol periods, where the channel is assumed flat fading and the channel gain is constant during two symbol periods.

In the study, the equivalent channel is considered, whose response includes the responses of the LED, optical channel and the photodiode (PD). Alamouti STBC should be implemented before OFDM modulation, where the channel is divided into parallel sub-channels in frequency domain and each sub-channel can be regarded as frequency-flat. On the other hand, because the frequency response of the LED is attenuated gradually with the frequency increase, the channel gains of the two consecutive subcarriers are different. To satisfy the Alamouti STBC transmission condition, the two symbol periods in our Alamouti STBC scheme are chosen from two consecutive OFDM symbols with the same subcarrier index, instead of two consecutive subcarriers in the same OFDM symbol, as shown in Fig.1.

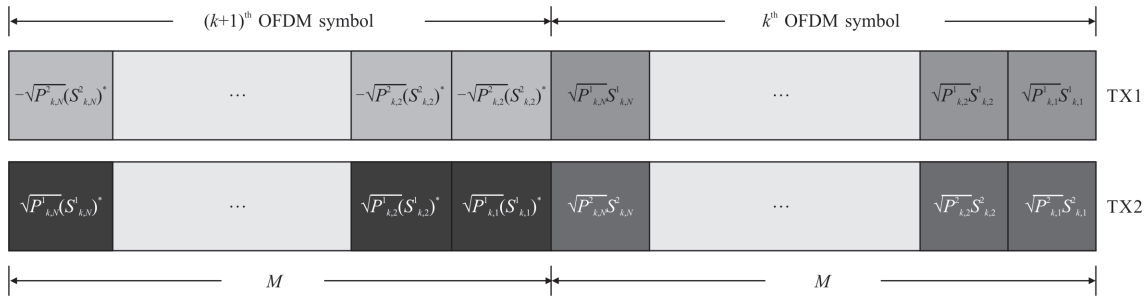


Fig.1 Alamouti STBC design

In this way, the received signals of the  $i$ th subcarrier in the consecutive OFDM symbols can be expressed as:

$$\begin{bmatrix} R_{k,i}^1 \\ R_{k+1,i}^1 \end{bmatrix} = \begin{bmatrix} \sqrt{P_{k,i}^1} S_{k,i}^1 & \sqrt{P_{k,i}^2} (S_{k,i}^2) \\ -\sqrt{P_{k,i}^2} (S_{k,i}^2)^* & \sqrt{P_{k,i}^1} (S_{k,i}^1)^* \end{bmatrix} \begin{bmatrix} H_{i,1} \\ H_{i,2} \end{bmatrix} + \begin{bmatrix} N_{k,i}^1 \\ N_{k+1,i}^1 \end{bmatrix} \quad (1)$$

$$\begin{bmatrix} R_{k,i}^2 \\ R_{k+1,i}^2 \end{bmatrix} = \begin{bmatrix} \sqrt{P_{k,i}^1} S_{k,i}^1 & \sqrt{P_{k,i}^2} (S_{k,i}^2) \\ -\sqrt{P_{k,i}^2} (S_{k,i}^2)^* & \sqrt{P_{k,i}^1} (S_{k,i}^1)^* \end{bmatrix} \begin{bmatrix} H_{i,3} \\ H_{i,4} \end{bmatrix} + \begin{bmatrix} N_{k,i}^2 \\ N_{k+1,i}^2 \end{bmatrix} \quad (2)$$

where  $R$  represents the received signals, the superscript denotes the PD number, the subscript  $k$  is the OFDM symbol number and  $i$  is the subcarrier number.  $S$  stands for the Alamouti coded signals as shown in Fig.1,  $P$  is the allocated power coefficient, and  $N$  is the zero-mean additive Gaussian noise.  $H_1, H_2, H_3$  and  $H_4$  denote the channel gain between the

two LEDs and the two PDs respectively.  $(\cdot)^*$  denotes the complex conjugate. Note that all the signals above are described in the frequency domain.

Although crosstalk exists in the MIMO channel, the channel can be easily de-correlated since the Alamouti STBC is designed orthogonally, which is then equivalent to two parallel channels. Through matrix conversion, the de-correlated channel can finally be denoted as

$$\begin{bmatrix} H_{i,1}^* & H_{i,2} \\ H_{i,2}^* & -H_{i,1} \end{bmatrix} \begin{bmatrix} R_{k,i}^1 \\ (R_{k+1,i}^1)^* \end{bmatrix} + \begin{bmatrix} H_{i,3}^* & H_{i,4} \\ H_{i,4}^* & -H_{i,3} \end{bmatrix} \begin{bmatrix} R_{k,i}^2 \\ (R_{k+1,i}^2)^* \end{bmatrix} = \begin{bmatrix} |H_{i,1}|^2 + |H_{i,2}|^2 + |H_{i,3}|^2 + |H_{i,4}|^2 & 0 \\ 0 & |H_{i,1}|^2 + |H_{i,2}|^2 + |H_{i,3}|^2 + |H_{i,4}|^2 \end{bmatrix} \begin{bmatrix} \sqrt{P_{k,i}^1} S_{k,i}^1 \\ \sqrt{P_{k,i}^2} (S_{k,i}^2) \end{bmatrix} + \begin{bmatrix} H_{i,1}^* & H_{i,2} \\ H_{i,2}^* & -H_{i,1} \end{bmatrix} \begin{bmatrix} N_{k,i}^1 \\ (N_{k+1,i}^1)^* \end{bmatrix} +$$

$$\begin{bmatrix} H_{i,3}^* & H_{i,4} \\ H_{i,4}^* & -H_{i,3} \end{bmatrix} \begin{bmatrix} N_{k,i}^2 \\ (N_{k+1,i}^2)^* \end{bmatrix} \quad (3)$$

Thereby, the signals are separated and estimated as follows

$$\hat{S}_{k,i}^1 = \frac{(H_{i,1})^* R_{k,i}^1 + H_{i,2} (R_{k+1,i}^1)^* + (H_{i,3})^* R_{k,i}^2 + H_{i,4} (R_{k+1,i}^2)^*}{(|H_{i,1}|^2 + |H_{i,2}|^2 + |H_{i,3}|^2 + |H_{i,4}|^2) \sqrt{P_{k,i}^1}} = S_{k,i}^1 + \frac{(H_{i,1})^* N_{k,i}^1 + H_{i,2} (N_{k+1,i}^1)^* + (H_{i,3})^* N_{k,i}^2 + H_{i,4} (N_{k+1,i}^2)^*}{(|H_{i,1}|^2 + |H_{i,2}|^2 + |H_{i,3}|^2 + |H_{i,4}|^2) \sqrt{P_{k,i}^1}} \quad (4)$$

$$\hat{S}_{k,i}^2 = \frac{(H_{i,2})^* R_{k,i}^1 - H_{i,1} (R_{k+1,i}^1)^* + (H_{i,4})^* R_{k,i}^2 - H_{i,3} (R_{k+1,i}^2)^*}{(|H_{i,1}|^2 + |H_{i,2}|^2 + |H_{i,3}|^2 + |H_{i,4}|^2) \sqrt{P_{k,i}^1}} = S_{k,i}^2 + \frac{(H_{i,2})^* N_{k,i}^1 - H_{i,1} (N_{k+1,i}^1)^* + (H_{i,4})^* N_{k,i}^2 - H_{i,3} (N_{k+1,i}^2)^*}{(|H_{i,1}|^2 + |H_{i,2}|^2 + |H_{i,3}|^2 + |H_{i,4}|^2) \sqrt{P_{k,i}^1}} \quad (5)$$

According to Eq.(4) and (5), the signal-to-noise ratios (SNRs) of the  $i$ th subcarrier for the two de-correlated channels can be computed by

$$\text{SNR}_{k,i}^1 = \frac{(|H_{i,1}|^2 + |H_{i,2}|^2 + |H_{i,3}|^2 + |H_{i,4}|^2) P_{k,i}^1}{N_0} \quad (6)$$

$$\text{SNR}_{k,i}^2 = \frac{(|H_{i,1}|^2 + |H_{i,2}|^2 + |H_{i,3}|^2 + |H_{i,4}|^2) P_{k,i}^2}{N_0} \quad (7)$$

where  $N_0$  is the noise power and we assume that the noise powers of the two receivers are equal.

As described above, since the frequency response of the LED is attenuated with the frequency increase, the PBA is further employed to combine with OFDM to optimize the communication parameters and improve the spectral efficiency. To achieve the maximum spectral efficiency, the PBA algorithm proposed in Reference [9] is introduced in, where power coefficient is obtained by maximizing the channel capacity. According to Eq.(3), we find that the original MIMO channel can be equivalent to the two de-correlated channels, and the SNRs of the two de-correlated channels are the same as each other, as shown in Eq.(6) and (7). As a result, the solutions of PBA for the two channels are totally the same.

Then the power allocation can be solved by maximizing the block channel capacity for each de-correlated channel under the power constraint, which can be written as

$$\begin{aligned} \max_{P_{k,1}, \dots, P_{k,M}} \sum_{i=1}^M C_i = \max_{P_{k,1}, \dots, P_{k,M}} \sum_{i=1}^M \log(1 + \text{SNR}_{k,i}) \\ \text{subject to } \sum_{i=1}^M P_{k,i} = M \quad P_{k,i} \geq 0 \end{aligned} \quad (8)$$

where  $C_i$  denotes the channel capacity of each de-correlated channel on  $i$ th sub-carrier,  $M$  is the number of sub-carrier and the total transmitted power is assumed to be equal to  $M$ .

Afterwards, given the target BER ( $\text{BER}_T$ ), the results of bit allocation, i.e. the modulation orders can be given by<sup>[9]</sup>

$$Q_{k,i} = 1 - \frac{1.5 \text{SNR}_{k,i}}{\log(5 \text{BER}_T)} \quad (9)$$

Considering that the constellation sizes of the quadrature amplitude modulation (QAM) signals must be powers of 2, finally the modulation orders should be rounded down to the nearest integer which is the powers of 2.

## 2 Experiment setup

Figure 2 and Figure 3 show the experimental setup and block diagram of the proposed MIMO-OFDM VLC system, respectively. In the experiment, transmitted signals are generated by an arbitrary function generator (AFG, Tektronix AFG3252C). Direct current (DC)

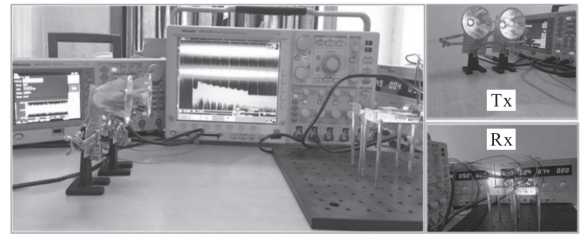


Fig.2 Experimental setup of the proposed MIMO-OFDM VLC system

supplied by AFG is also added to ensure that the transmitted signals are positive. Then the mixed signals are transmitted through the LEDs in the form of optical power. At the receiver, the optical signals are focused on the PDs and converted into electrical signals. Since light from a single transmitter will reach multiple receivers, crosstalk exists among co-located channels. The superimposed signals are recorded by a

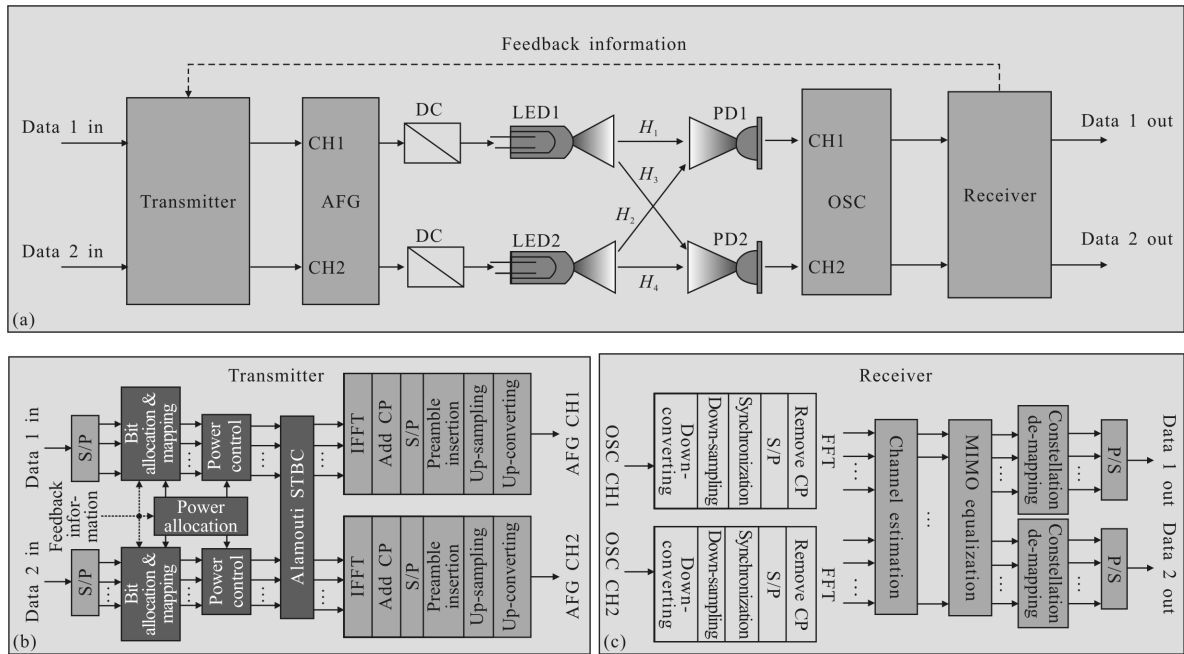


Fig.3 Block diagram of the proposed MIMO-OFDM VLC system(a), block diagram of transmitter (b), block diagram of receiver (c)

commercial high-speed digital oscilloscope (OSC, Tektronix MSO4104) and then sent for demodulation. Two commercially available LEDs (Cree XLamp XP-E) radiating red light are used as the transmitters, whose center wavelengths are 620 nm. Two PD modules (Hamamatsu C12702 -11, 0.42 A/W responsivity at 620 nm) with 1 mm<sup>2</sup> active area and about 100 MHz bandwidth are used as the receivers.

At the transmitter, two streams of random binary input data are converted into parallel sub-streams separately, each sub-stream corresponds to a frequency-flat sub-channel in the OFDM system. Power is allocated to each sub-channel, according to the feedback of channel SNR. Different bits are decided for sub-channels by the allocated power, the channel SNR and the target BER. Then parallel binary sub-streams are mapping to QAM signals according to the bit allocation. Power control is performed based on the results of power allocation to adjust the power of the sub-channels. Afterwards, Alamouti STBC is encoded and OFDM symbols are generated by inverse fast Fourier transform (IFFT). Cyclic prefix (CP) is attached to each OFDM symbol to overcome the ISI. After OFDM modulation, parallel sub-streams are

converted to serial data streams and two transmitted data streams are recovered. Two orthogonal preambles are generated and inserted in front of the data streams separately, which are required for synchronization and channel estimation at the receiver. Finally, data streams are up-sampled and up-converted to a certain carrier, by which complex-to-real-value conversion is conducted and real-value OFDM symbols are generated<sup>[17]</sup>.

At the receiver, the demodulation is performed with offline signal processing, which is the inverse process of the signal modulation at the transmitter. DC is firstly removed from the received signals. After down-converting and down-sampling, complex-value symbols are recovered. Frame synchronization is required to detect the starting position of each data stream by preamble. CP is removed from each OFDM symbol, which is then demodulated by fast Fourier transform (FFT). After OFDM demodulation, parallel MIMO sub-systems are obtained again in frequency domain. Channel gain is estimated in frequency domain, which is required for MIMO equalization and PBA. After MIMO equalization, channel crosstalk is eliminated and the Alamouti STBC symbols are decoded, where symbols are combined across the time

and the space dimensions. Finally, constellation demapping is carried out and two binary data streams are recovered.

### 3 Results discussion

In this section, the performance of the proposed MIMO-OFDM VLC system is examined. The system parameters configured in the experiment are listed in Tab.1.

**Tab.1 System parameters**

System parameters	Values
Bandwidth/MHz	12.5
Up-converted frequency/MHz	8.75
Subcarrier number	256
Up-sampling rate	4
Distance between transmitters and receivers/cm	80

Firstly, the measured amplitude frequency responses of MIMO VLC channel are shown in Fig.4, where  $|H_i| (i=1, 2, 3, 4)$  represents the channel gain from the LED to the PD as depicted in Fig.3. Here, the channel is actually the equivalent one which consists of the responses of the LED, optical channel and the PD, and is estimated by least square (LS) algorithm in frequency domain. As shown in Fig.4, the frequency response of the equivalent channel is strongly attenuated at high frequencies.

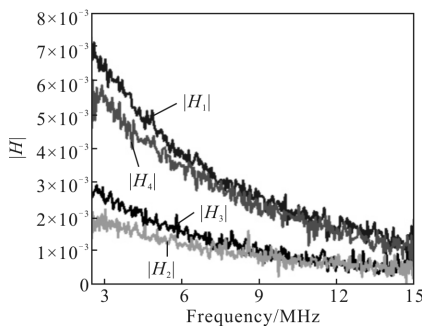


Fig.4 Measured amplitude frequency responses of the MIMO VLC channel

In order to measure the channel correlation, the matrix condition number  $KD$  is introduced, which

reflects the correlation of the MIMO channel<sup>[18]</sup>. By using OFDM modulation, the channel is divided into several sub-channels, which results in parallel MIMO sub-systems in the frequency domain; therefore, the value of  $KD$  here is the averaged matrix condition number over all the MIMO sub-systems. As previous discussion, the results of power and bit allocation for two data streams are the same. For each data stream, the power and bit allocation results in condition of  $BER_T=0.003$  and  $K_D=3.0$  are depicted in Fig.5. The SNR of each subcarrier is also given in Fig.5. The simulation results show that more power is allocated to the subcarriers with higher SNR; as a result, those subcarriers are also assigned with higher modulation orders to achieve higher channel capacity.

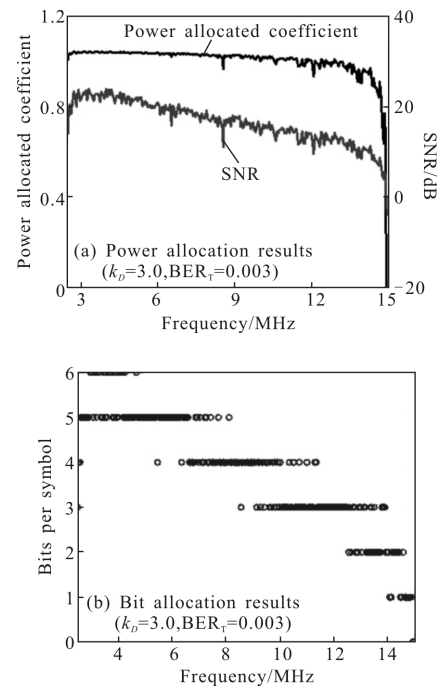


Fig.5 Power and bit allocation results ( $K_D=3.0, BER_T=0.003$ )

The advantage of the PBA is explained by data rate comparisons between STBC based MIMO-OFDM VLC system with and without PBA, which is shown in Fig.6. In order to make the experimental results comparable, total transmitted power for all the experiments are kept the same. The solid curve filled triangles in the figure stands for the data rates of the system without PBA. Each point represents the



performance of a certain modulation type, plotted with data rate on the horizontal axis and BER on the vertical. By increasing the modulation orders, the data rates are also improved; however the BER performance is decreased. Solid curve filled triangles depicts BER versus data rate for the system with PBA. Each point represents the performance based on a certain target BER, plotted with data rate on the horizontal axis and BER on the vertical. Given the higher target BER, the higher modulation orders would be allocated according to Eq. (9). Therefore, the data rates are also increased. As can be seen, the data rates of the system with PBA can achieve up to 37, 39 and 41 Mbit/s when the target BERs are equal to 0.001, 0.002 and 0.004. Considering the 7% pre-FEC threshold of  $3.8 \times 10^{-3}$ , the target BERs are set as 0.001, 0.002, 0.003 and 0.004 in the experiments. Then the measured BERs of the system with PBA are all below the threshold as shown in Fig.6; while the BER performance of the system without PBA is much worse, even in the 4 QAM modulated system. The experimental results also confirm that the data rates of the system with PBA are higher than the system without PBA under the same BER level. When the target BER is set to 0.004, the data rate of the system with PBA is 41 Mbit/s; however, the data rate of the system without PBA using fixed 4QAM modulation is only 22 Mbit/s under the similar BER level, which is obviously much lower.

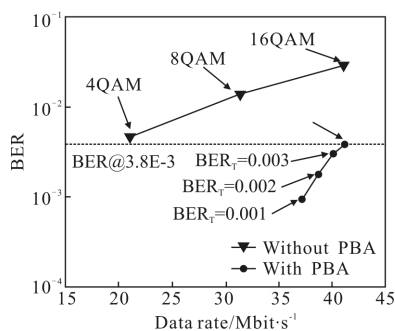


Fig.6 Data rate comparisons between systems with and without PBA ( $K_D=3.0$ )

Figure 7 shows data rates of the system with

different channel correlations. Two solid curves depict the data rates of the proposed system with PBA in condition of different target BERs. The dashed curve shows the data rates of the STBC based MIMO-OFDM VLC system using fixed modulation type of 8QAM. The results indicate that the data rates change little when the channel correlations are increased, which prove that the STBC is robust to channel correlation.

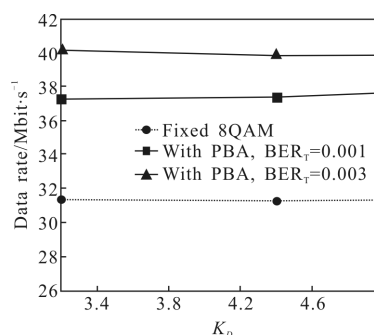


Fig.7 Data rates with different channel correlations

## 4 Conclusions

In conclusion, we have proposed and experimentally demonstrated an adaptive STBC MIMO-OFDM VLC system. In the system, Alamouti STBC is introduced to provide reliable transmission, which is proved to be robust to channel correlation. Meanwhile, PBA is combined with the STBC MIMO-OFDM system to further improve the spectral efficiency. Experimental results confirm the theoretical analysis, and show that the data rates can be greatly increased.

## References:

- [1] Pathak P H, Feng X, Hu P, et al. Visible light communication, networking, and sensing: a survey, potential and challenges [J]. *IEEE Communications Surveys & Tutorials*, 2015, 17(4): 2047-2076.
- [2] Shen Zhenmin, Lan Tian, Wang Yun. Simulation and analysis for indoor visible-light communication based on LED [J]. *Infrared and Laser Engineering*, 2015, 44 (8): 2496-2500. (in Chinese)
- [3] Mesleh R, Elgala H, Haas H. Optical spatial modulation [J]. *IEEE/OSA Journal of Optical Communications &*

- Networking*, 2011, 3 (3): 234–244.
- [4] Chi N, Wang Y, Wang Y, et al. Ultra high speed single red-green-blue light-emitting diode based visible light communication system utilizing advanced modulation formats [J]. *Chinese Optics Letters*, 2014, 12(1): 22–25.
- [5] Huang X, Wang Z, Shi J, et al. 1.6 Gbit/s phosphorescent white LED based VLC transmission using a cascaded pre-equalization circuit and a differential outputs PIN receiver [J]. *Optics Express*, 2015, 23(17): 22034–22042.
- [6] Deng L, Fan Y. Research on the performance of indoor visible light non-DC-biased OFDM system based on color/frequency/space three-dimension resources multiplexing [J]. *Infrared and Laser Engineering*, 2016, 45 (7): 0722002. (in Chinese)
- [7] Wang Y, Chi N, Wang Y, et al. High-speed quasi-balanced detection OFDM in visible light communication [J]. *Optics Express*, 2013, 21(23): 27558–27564.
- [8] Bykhovsky D, Arnon S. An experimental comparison of different bit-and-power-allocation algorithms for DCO – OFDM [J]. *Journal of Lightwave Technology*, 2014, 32(8): 1559–1564.
- [9] Guo X, Li X. Experimental demonstration of an adaptive orthogonal frequency division multiplexing visible light communication system [J]. *Chinese Optics Letters*, 2016, 14 (11): 23–27.
- [10] Wang Y, Chi N. Demonstration of high-speed 2×2 non-imaging MIMO Nyquist single carrier visible light communication with frequency domain equalization [J]. *Journal of Lightwave Technology*, 2014, 32(11): 2087–2093.
- [11] Zeng L, O’ Brien D C, Minh H L, et al. High data rate multiple input multiple output (MIMO) optical wireless communications using white LED lighting [J]. *IEEE Journal on Selected Areas in Communications*, 2009, 27(9): 1654–1662.
- [12] Hong Y, Wu T, Chen L. On the performance of adaptive MIMO-OFDM indoor visible light communications[J]. *IEEE Photonics Technology Letters*, 2016, 28(8): 907–910.
- [13] Uysal M, Georgiades C N. Effect of spatial fading correlation on performance of space-time codes [J]. *Electronics Letters*, 2001, 37(3):181–183.
- [14] Wei C, Wu F, Chen Z, et al. Indoor VLC system with multiple LEDs of different path lengths employing space-time block-coded DMT/CAP modulation [J]. *IEEE/OSA Journal of Optical Communications & Networking*, 2015, 7 (3): 459–466.
- [15] Simon M K, Vlnrotter V A. Alamouti-type space-time coding for free-space optical communication with direct detection[J]. *IEEE Transactions on Wireless Communications*, 2005, 4(1): 35–39.
- [16] Shi J, Wang Y, Chi N, et al. Enhanced performance using STBC aided coding for LED –based multiple input single output visible light communication network [J]. *Microwave & Optical Technology Letters*, 2015, 57(12): 2943–2946.
- [17] Wang Y, Wang Y, Chi N. Experimental verification of performance improvement for a gigabit wavelength division multiplexing visible light communication system utilizing asymmetrically clipped optical orthogonal frequency division multiplexing [J]. *Photonics Research*, 2014, 2(5): 138–142.
- [18] Heath R W, Paulraj A J. Switching between diversity and multiplexing in MIMO systems [J]. *IEEE Transactions on Communications*, 2005, 53(6): 962–968.